Nanoelectromechanics of Methylated DNA in a Synthetic Nanopore

U. Mirsaidov,[†] W. Timp,[‡] X. Zou,[†§] V. Dimitrov,[†] K. Schulten,[†] A. P. Feinberg,[‡] and G. Timp[†]
[†]Beckman Institute, University of Illinois at Urbana-Champaign, Urbana, Illinois; [‡]School of Medicine, The Johns Hopkins University, Baltimore, Maryland; and [§]School of Physics, Peking University, Beijing, China

ABSTRACT Methylation of cytosine is a covalent modification of DNA that can be used to silence genes, orchestrating a myriad of biological processes including cancer. We have discovered that a synthetic nanopore in a membrane comparable in thickness to a protein binding site can be used to detect methylation. We observe a voltage threshold for permeation of methylated DNA through a <2 nm diameter pore, which we attribute to the stretching transition; this can differ by >1 V/20 nm depending on the methylation level, but not the DNA sequence.

Received for publication 8 September 2008 and in final form 2 December 2008.

*Correspondence: gtimp@uiuc.edu

Some of the cytosine residues in all vertebrate genomes are methylated, producing what amounts to a fifth DNA base, 5-methylcytosine (1). Methylation adds information not encoded in the DNA sequence, but it does not interfere with the Watson-Crick pairing—the methyl group is positioned in the major groove of the DNA. The pattern of methylation controls protein binding to target sites on DNA, affecting changes in gene expression and in chromatin organization, often silencing genes, which physiologically orchestrates processes like differentiation, and pathologically leads to cancer (1). Although DNA methylation has a profound effect on biological functions by affecting protein binding, the actual mechanism that affects binding is still mysterious. The structure of methylated DNA inferred from x-ray diffraction and nuclear magnetic resonance indicates that the effect of methylation on the conformation of DNA is very subtle, and localized near the methylation site (2). On the other hand, the DNA dynamics at the methylation site seem to be dramatically reduced—i.e., the molecule gets stiffer (3). Molecular dynamics (MD) simulations indicate that the methyl groups reduce the DNA flexibility because of steric hindrance (the methyl groups are bulky) and because the DNA folds around it (they're also hydrophobic) (4).

The prospects of using DNA methylation as a molecular diagnostic in medicine are stymied by limitations of the technology used for detection. Immunoprecipitation of methylated DNA or methylation-sensitive restriction digestion represent the state-of-the-art for discriminating methylated from unmethylated DNA. Immunoprecipitation suffers a lack of sensitivity, causing the technique to be sensitive only to large changes in methylation. Methyl-sensitive restriction digestion requires relatively long intact DNA fragments and is limited to CpGs in recognition sites.

Here, we report measurements of the permeation of methylated DNA through a synthetic nanopore, using an electric field to force single molecules to translocate across the membrane through the pore. The diameter of the pore is so small that molecules can only move through it one at a time, while the thin membrane (~20 nm) offers the opportunity to test the electromechanical properties of methylated DNA of a size comparable to a protein-binding site (3–10 nm). For pores <2.0 nm in diameter—smaller than the DNA helix—we find a voltage threshold for permeation of DNA that depends on the methylation level.

We studied two fragments of genomic DNA that are known to control expression based on methylation status: MS3 and BRCA1. MS3 is one of the CTCF binding sites of the *Igf2* imprinting control region (5). Methylation of MS3 prevents CTCF binding, allowing an enhancer to reach *Igf2* and turn on expression. Aberrant hypermethylation causes elevated expression of *Igf2*, which has been shown to encourage cancer. In contrast, *BRCA1* is a tumor suppressor gene used to repair DNA. Methylation of the *BRCA1* promoter causes binding of a protein (MeCP2) that inhibits expression leading to mutations and breast/ovarian cancer (6).

The fabrication of synthetic nanopores in Si_3N_4 membranes has been described in detail elsewhere (7). The insets to Fig. 1, *b* and *c* show transmission electron micrographs, taken at a tilt angle of 0°, of roughly circular pores with apparent diameters of $d = 1.8 \pm 0.2$ nm and 1.7 ± 0.2 nm in membranes 22 ± 3-nm and 17 ± 3-nm thick, respectively. Using images taken at different tilt angles, we model the pore geometry as two intersecting cones each with >15–20° cone angle. We characterized electrolytic conductance for each pore; a line fit to the data for voltages <0.5 V (see the Supporting Material) yields 553 ± 6 pS and 470 ± 9 pS for the pores shown in the insets to Fig. 1, *c* and *d*, respectively. Next, we tested the electric-field-driven permeability of DNA through the pore using a membrane transport bi-cell consisting of a two-chamber piece of acrylic with the nitride membrane separating two compartments, each containing electrolyte and an Ag/AgCl

Editor: Alberto Diaspro.

doi: 10.1016/j.bpj.2008.12.3760

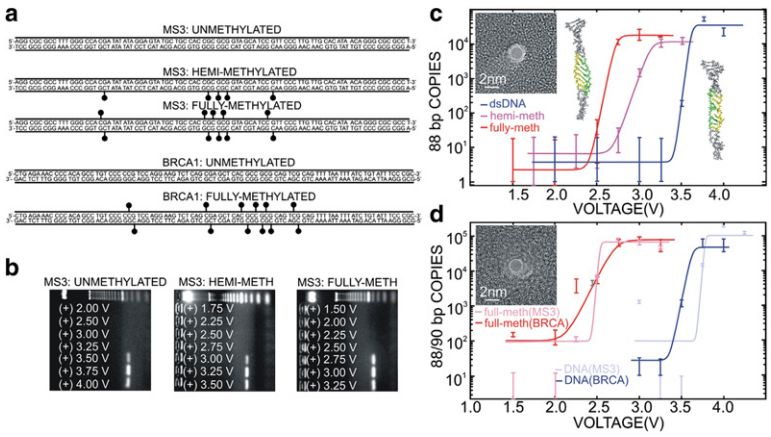

FIGURE 1 Threshold voltage for DNA permeation through a synthetic nanopore depends on methylation. (*a*) Methylation patterns in *MS3* and *BRCA1*. The methylated CpG sites on each strand are attached to solid circles. (*b*) Gel electrophoresis arrays with eight horizontal lanes indicating *MS3* found at the positive (+) electrode in the *trans* compartment of a bi-cell with a Si_3N_4 membrane containing a 1.8-nm pore (in *c*) separating the two chambers. A 25-bp ladder in the top lane is used for gel calibration. Below that, the voltage bias across the membrane identifies the lane. Unmethylated, hemimethylated, and fully methylated *MS3* permeate the pore for voltages $V > 3.25$, $V > 2.75$ V, and $V > 2.5$ V, respectively. (*c*) qPCR results indicating the number of *MS3* DNA copies that permeate through the 1.8 ± 0.2 nm pore shown in the inset (*left*) as a function of the membrane voltage. The solid lines represent a fit to the data. In correspondence with the gels, unmethylated, hemimethylated, and fully methylated MS3 permeate the 1.8-nm pore above a threshold of $U = 3.6$ V, $U = 3.2$ V, and $U = 2.7$ V, respectively. (*Inset*, *middle* and *right snapshots*) Methylated and unmethylated *MS3* translocating through the 1.8-nm pore. Both DNA exhibit an ordered B-DNA form, but there is a significant degree of disorder for unmethylated DNA. The highlighted region of the strand shows the portion of the DNA where methylated cytosines are located. The same region is also highlighted in the unmethylated strand for comparison. (*d*) qPCR results indicating the number of *MS3* and *BRCA1* DNA copies that permeate through the 1.7 ± 0.2 nm pore shown in the inset as a function of the membrane voltage. The solid lines represent a fit to the data. Unmethylated *MS3* and *BRCA1* permeate at $U > 3.8$ V and $U > 3.6$ V, respectively, while the threshold for fully methylated MS3 and BRCA1 are $U = 2.5$V and $U = 2.7$V, respectively.

electrode (Warner Instruments, Hamden, CT). The bi-cell used for the transport experiments was filled with 100 mM KCl electrolytic solution, buffered to pH ~ 8 with 10 mM Tris-HCl. We then injected a concentration of 10^9 molecules/μL into the cathode chamber of the bi-cell, applied a voltage across the membrane using Ag/AgCl electrodes, and monitored the current through the pore for 3 h. We have previously reported that voltage-driven translocations of DNA cause a temporary blockade of the open pore current (8). However, for the electric fields used in these experiments the translocation velocity is supposed to be >1 bp/μs, approaching 1 bp/10 ns, corresponding to <10 μs current transients (9). On the other hand, the membrane capacitance (>400 pF) in conjunction with the resistance due to the electrolyte (>10 kΩ) limits the response time of the nanopore, precluding observation of transients shorter than ~10 μs. So, to unambiguously establish that the DNA injected at the cathode permeates a pore, we assayed the sample from the anode using either PCR amplification followed by agarose gel electrophoresis or real-time quantitative polymerase chain reaction (qPCR) as described in detail elsewhere (8). For agarose gel electrophoresis, the DNA was first concentrated and then amplified with a kit from Invitrogen (Carlsbad, CA) using primers from IDT (Coralville, IA), finally run on an agarose gel. Alternatively, concentrated anode DNA was analyzed by qPCR using the SYBR Green kit (Invitrogen). qPCR is used prevalently as the standard for DNA quantitation and considered to be highly reliable (10).

We investigated the permeability of *MS3* and *BRCA1* with different methylation levels and profiles through two pores with similar (1.8 nm) diameters. The patterns of methylated CpG sites in the five strands used here are shown in Fig. 1 *a*. The gel arrays shown in Fig. 1 *b* illustrate permeability of the 1.8-nm pore shown in the inset to Fig. 1 *c* as a function of the voltage applied across the membrane. The left gel indicates a threshold voltage for permeation of unmethylated DNA $V > 3.25$ V. We have previously reported similar phenomena and used MD to interpret the threshold as evidence of the stretching transition in DNA (8). The electric force on the DNA in a synthetic nanopore drops abruptly away from the center of the membrane, z_0, according to

$$F(z) \sim (bV/\pi L_{\mathrm{mem}}) \times 1/(1 + (b(z - z_0)/L_{\mathrm{mem}}))^2,$$

where L_{mem} denotes the membrane thickness, z-z_0 represents the distance from the center of the membrane along the axis of the pore, V denotes the applied voltage bias across the membrane, and b is a geometric factor (8). At low voltage, the DNA penetrates the bi-conical pore to a diameter of ~2.5 nm, where the translocation stalls. At threshold, the differential force acting on the leading nucleotides is sufficient (~60 pN) to stretch the helix toward the center of the membrane. As it stretches, the force on the leading edge increases, pulling the DNA through the pore.

The other gel arrays shown in Fig. 1 *b* indicate that the same pore can be used to discriminate fully methylated and hemimethylated from unmethylated DNA. Notice that the threshold voltages for permeation of fully and hemimethylated DNA through the 1.8-nm pore is $V > 2.5$ V and $V > 2.75$ V, respectively—both smaller than the threshold for unmethylated DNA. The voltage thresholds inferred from these gels are corroborated by separate qPCR experiments on the same pore. Fig. 1 *c* represents the results of three qPCR analyses—one for unmethylated, one for hemi-, and another for fully methylated DNA—showing the number of DNA copies translocating through the pore as a function of the applied potential.

Generally, we observe that the amount of DNA that permeates the pore rises abruptly over a range of ~250 mV

near a threshold that is especially sensitive to the DNA methylation level. The permeation rate can essentially be described by the transition-state relation of the Kramers type,

$$R = R_0/(1 + \exp[q^*(V - U)/kT]),$$

where R_0 is a frequency factor, q^*U is the effective barrier height, q^*V is the reduction in the energy barrier due to the applied potential, and kT represents the thermal energy (11). Using these relations and accounting for the qPCR baseline, the data was fit; the results are overlaid on the scatter plots in Fig. 1.

The threshold voltages for fully and hemimethylated MS3 are consistently below that observed for the unmethylated strand and easily resolved. For example, the threshold for unmethylated *MS3* in Fig. 1 *c* is U~3.6 V, whereas hemi- and fully methylated *MS3* show a threshold of $U = 3.2$ V and 2.7 V, respectively. The change in threshold is also consistent with features observed in MD simulations of the translocation of DNA strands. Snapshots of the DNA in the pore shown in Fig. 1 *c* reveal the molecular structure with atomic detail, indicating that both methylated and unmethylated DNA exhibit a B-form, but methylated DNA is more ordered. The preservation of the B-form in methylated DNA is also evident in the root mean-square deviation in the helix diameter. At 4 V, the interior segments of methylated and unmethylated DNA have a root mean-square deviation 0.29 nm and 0.49 nm, respectively. Correspondingly, the translocation velocity of the methylated MS3 through the pore at 4 V is higher (1.0 nm/ns) than unmethylated (0.8 nm/ns).

Though the threshold is apparently related to the methylation level, it is relatively insensitive to the DNA sequence, as evident from the comparison between the permeation of *MS3* and *BRCA1* through a 1.7 $\pm$ 0.2-nm pore shown in Fig. 1 *d*. The *BRCA1* and *MS3* sequences are different, but the thresholds for stretching are similar: $U = 3.6$ V and 3.8 V, respectively. Yet fully methylated *BRCA1*, which has 12 methylated CpG sites, and fully methylated *MS3*, which has comparable number—10—both show a similar shift in threshold to $U =$ 2.7 V and 2.5 V, respectively. The large shifts in the thresholds with methylation (which appear to be only weakly dependent on sequence) are surprising because the leading nucleotides in the strand are separated by a distance $>$18 bp (~6 nm) from any methylation site, which is comparable to the length of a protein binding site.

For the first time, to our knowledge, we have demonstrated a sensitive means to detect the covalent modification of DNA by methylation of cytosines from measurements of the change in the electromechanical properties of the DNA strand. Due to the biconical nature of the pore, the electric field is focused near the central 4 nm of the membrane, which is comparable to a protein-binding site. How proteins specifically recognize methylation is still controversial, but proteins like the methyl-binding protein MeCP2 must encounter DNA electromechanics similar that seen in these synthetic pores. Based on gel mobility shift assays, the effect of methylation is supposed to be local to the methylation site (12), but our data indicates that the effect of methylation affects the electromechanics of the leading edge of a DNA strand at least 18-bp away. Thus, methylation markers may affect protein binding to DNA on the same scale. And finally, this technology also has the potential to be used as a sieving technique, to separate DNA based on methylation. This could have potential applications in epigenetic analysis, replacing existing technologies such as MeDIP or HELP.

SUPPORTING MATERIAL

Current-voltage characteristcs and a figure are available at http://www.biophysj.org/biophysj/supplemental/S0006-3495(08)04004-6.

ACKNOWLEDGMENTS

We gratefully acknowledge discussions with A. Aksimentiev and B. Dorvel.

We acknowledge the use of the Center for Microanalysis of Materials, supported by the United States Department of Energy grant No. DEFG02-91-ER45439. This work was funded by National Institutes of Health grant Nos. R01 HG003713A and P41-RR05969, and National Science Foundation grant No. TH 2008-01040 ANTC; it was also partially supported by National Institutes of Health grant No. CA65145.

REFERENCES and FOOTNOTES

1. Brena, R. M., T. H. M. Huang, and C. Plass. 2006. Toward a human epigenome. *Nat. Genet.* 38:1359–1360.
2. Heinemann, U., and M. Hahn. 1992. CCAGGC-m5C-TGG. Helical fine structure, hydration, and comparison with CCAGGCCTGG. *J. Biol. Chem.* 267:7332–7341.
3. Nathan, D., and D. M. Crothers. 2002. Bending and flexibility of methylated and unmethylated *Eco*RI DNA. *J. Mol. Biol.* 316:7–17.
4. Derreumaux, S., M. Chaoui, G. Tevanian, and S. Fermandjian. 2001. Impact of CpG methylation on structure, dynamics and solvation of cAMP DNA responsive element. *Nucleic Acids Res.* 29:2314–2326.
5. Bell, A. C., and G. Felsenfeld. 2000. Methylation of a CTCF-dependent boundary controls imprinted expression of the Igf2 gene. *Nature.* 405:482–485.
6. Catteau, A., and J. R. Morris. 2002. BRCA1 methylation: a significant role in tumor development? *Semin. Cancer Biol.* 12:359–371.
7. Ho, C., R. Qiao, J. B. Heng, A. Chatterjee, R. J. Timp, et al. 2005. Electrolytic transport through a synthetic nanometer-diameter pore. *Proc. Natl. Acad. Sci. USA.* 102:10445–10450.
8. Heng, J. B., A. Aksimentiev, C. Ho, P. Marks, Y. V. Grinkova, et al. 2006. The electromechanics of DNA in a synthetic nanopore. *Biophys. J.* 90:1098–1106.
9. Aksimentiev, A., J. B. Heng, G. Timp, and K. Schulten. 2004. Microscopic kinetics of DNA translocation through synthetic nanopores. *Biophys. J.* 87:2086–2097.
10. Bookout, A. L., C. L. Cummins, D. J. Mangelsdorf, J. M. Pesola, and M. F. Kramer. 2006. High-throughput real-time quantitative reverse transcription PCR. *In* Current Protocols in Molecular Biology, Chapt. 15:Unit 15.18. Howard Hughes Medical Institute, University of Texas Southwestern Medical Center, Dallas, TX.
11. Goychuk, I., and P. Hanggi. 2002. Ion channel gating: a first-passage time analysis of the Kramers type. *Proc. Natl. Acad. Sci. USA.* 99:3552–3556.
12. Fraga, M. F., E. Ballestar, G. Montoya, P. Taysavang, P. A. Wade, et al. 2003. The affinity of different MBD proteins for a specific methylated locus depends on their intrinsic binding properties. *Nucleic Acids Res.* 31:1765–1774.